

## Supporting Information for

# Binding properties of mono- and dimeric pyridine dicarboxamide ligands to human telomeric higher-order G-quadruplex structures

C. Saintomé, P. Alberti, N. Guinot, P. Lejault, J. Chatain, P. Mailliet, J.-F. Riou and A. Bugaut\*

<sup>a</sup> “Structure and Instability of Genomes” laboratory, Sorbonne Universités, Muséum National d’Histoire Naturelle, Inserm U1154, CNRS UMR 7196, 75005 Paris, France. <sup>b</sup> UPMC Paris 6 Université, 75005 Paris, France. \*Corresponding author: abugaut@mnhn.fr

## Table of contents

<b>Supplementary tables and figures.....</b>	<b>2</b>
<b>Table S1</b> Sequences of the oligonucleotides used in this study.	
<b>Table S2</b> Calculated and obtained experimental values of the ligand-to-G4 unit molar ratios	
<b>Table S3</b> UV-melting temperatures of the complexes formed between the oligonucleotides and the ligands.	
<b>Fig. S1</b> (A) FRET melting curves of F21T in the presence of (A) 1 $\mu$ M of 360A, (B) 0.5 $\mu$ M and (C) 1 $\mu$ M of (360A) <sub>2A</sub> , without or with 3 $\mu$ M or 10 $\mu$ M of double-stranded competitor ds26.(B) Representative FRET melting curves of H69Q1 in the presence of 1.5 $\mu$ M of (360A) <sub>2A</sub> without or with 10 $\mu$ M of double-stranded competitor ds26. (C) FRET melting temperatures of H69Q1,Q2,Q3 in presence of 1.5 $\mu$ M of (360A) <sub>2A</sub> without or with 10 $\mu$ M of ds26.	
<b>Fig. S2</b> Changes in the CD spectra and changes in the maximum CD value of H21, H45 and H69 upon addition of increasing amounts of (360A) <sub>2A</sub> in 10 mM lithium cacodylate pH 7.2, 10 mM KCl, 90 mM LiCl.	
<b>Fig. S3</b> Changes in the CD spectrum and changes in the maximum CD value of H45 upon addition of increasing amounts of 360A and (360A) <sub>2A</sub> .	
<b>Fig. S4</b> Changes in the CD spectrum and changes in the maximum CD value of H93 upon addition of increasing amounts of 360A and (360A) <sub>2A</sub> .	
<b>Fig. S5</b> Changes in the CD spectra and the maximum CD values of H45(TTA) <sub>3</sub> and H69(TTA) <sub>3</sub> in 10 mM lithium cacodylate pH 7.2, 100 mM NaCl.	
<b>Fig. S6</b> (A) Percentage of inhibition of RPA binding to telomeric oligonucleotide substrate H45 in the presence of increasing concentrations of 360A or (360A) <sub>2A</sub> for 5 min prior to incubation with RPA for 20 min. (B) Percentage of displacement of RPA from the telomeric oligonucleotide substrate H45 upon addition of increasing amounts of 360A or (360A) <sub>2A</sub> .	
<b>Fig. S7</b> (A) Percentage of inhibition of RPA binding to telomeric oligonucleotide substrate H69 with 5 $\mu$ M of 360A or 2.5 $\mu$ M of (360A) <sub>2A</sub> for 5 min in the presence of double-stranded competitor ds26 prior to incubation with RPA for 20 min. (B) Percentage of displacement of RPA from the telomeric oligonucleotide substrate H69 (20 min incubation) in the presence of double-stranded competitor ds26 upon addition of 5 $\mu$ M of 360A or 2.5 (360A) <sub>2A</sub> $\mu$ M for 5 min.	
<b>Fig. S8</b> (A) Percentage of inhibition of RPA binding to mutated telomeric oligonucleotide substrates H27mut, H51mut and H75mut in the presence of increasing concentrations of 360A or (360A) <sub>2A</sub> for 5 min prior to incubation with RPA for 20 min. (B) Percentage of displacement of RPA from the mutated telomeric oligonucleotide substrates H27mut, H51mut and H75mut upon addition of increasing amounts of 360A or (360A) <sub>2A</sub> .	
<b>Materials and methods.....</b>	<b>11</b>
<b>References.....</b>	<b>14</b>

**Table S1:** Sequences of the oligonucleotides used in this study

Sequence name	Number of G4 unit	Sequence (5' to 3')
H21	1	(GGGTTA) <sub>3</sub> GGG
H45	2	(GGGTTA) <sub>7</sub> GGG
H69	3	(GGGTTA) <sub>11</sub> GGG
H93	4	(GGGTTA) <sub>15</sub> GGG
H45(TTA) <sub>3</sub>	2	(GGGTTA) <sub>3</sub> GGG(TTA) <sub>3</sub> (GGGTTA) <sub>3</sub> GGG
H69(TTA) <sub>3</sub>	3	[(GGGTTA) <sub>3</sub> GGG(TTA) <sub>3</sub> ] <sub>2</sub> (GGGTTA) <sub>3</sub> GGG
H27mut	0	TTAGGCTTACGGTTAGCGTTACGGTTA
H51mut	0	TTAGGCTTACGGTTAGCGTTACGGTTAGGCTTACGGTTAGCGTTACGGTTA
H75mut	0	TTAGGCTTACGGTTAGCGTTACGGTTAGGCTTACGGTTAGCGTTACGGTTAGGCTTACGGTTAGCGTTACGGTTA
ds26	0	CAATCGGATCGAATTCGATCCGATTG

**Table S2:** Calculated theoretical and obtained experimental values of the ligand to G4 unit molar ratios

Oligonucleotide	Number of G4 unit (n <sub>G4</sub> )	Number of TTA linker (n <sub>TTA</sub> )	360A		(360A) <sub>2A</sub>	
			Cal. <sup>a</sup>	Exp.	Cal. <sup>a</sup>	Exp.
H21	1	0	2.00	1.87 ± 0.13	1.00	1.22 ± 0.12
H45	2	1	2.50	2.52 ± 0.18	1.50	1.55 ± 0.08
H69	3	2	2.67	2.74 ± 0.08	1.67	1.63 ± 0.07
H93	4	3	2.75	2.71 ± 0.11 <sup>b</sup>	1.75	1.66 ± 0.06 <sup>b</sup>

<sup>a</sup> Theoretical ligand/G4 unit molar ratio values were calculated as:

$(2 \cdot n_{G4} + n_{TTA}) / n_{G4}$ , for 360A and  $(n_{G4} + n_{TTA}) / n_{G4}$ , for (360A)<sub>2A</sub>

<sup>b</sup> Experimental data for H93 are presented in Figure S4

**Table S3:** Apparent UV-melting temperatures (*T<sub>m</sub>*<sub>APP</sub>) of the complexes formed between the oligonucleotides and the G4 ligands

Oligonucleotide (concentration)	<i>T<sub>m</sub></i> (°C)	<i>T<sub>m</sub></i> <sub>APP</sub> (°C) <sup>a</sup>	
	DNA	DNA + 360A (2eq. G4)	DNA + (360A) <sub>2A</sub> (1eq. G4)
H21 (3 μM)	60	64	70
H45 (1.5 μM)	53	70	73
H69 (1 μM)	47	70	74

<sup>a</sup> Values are given with an experimental error of ± 1°C

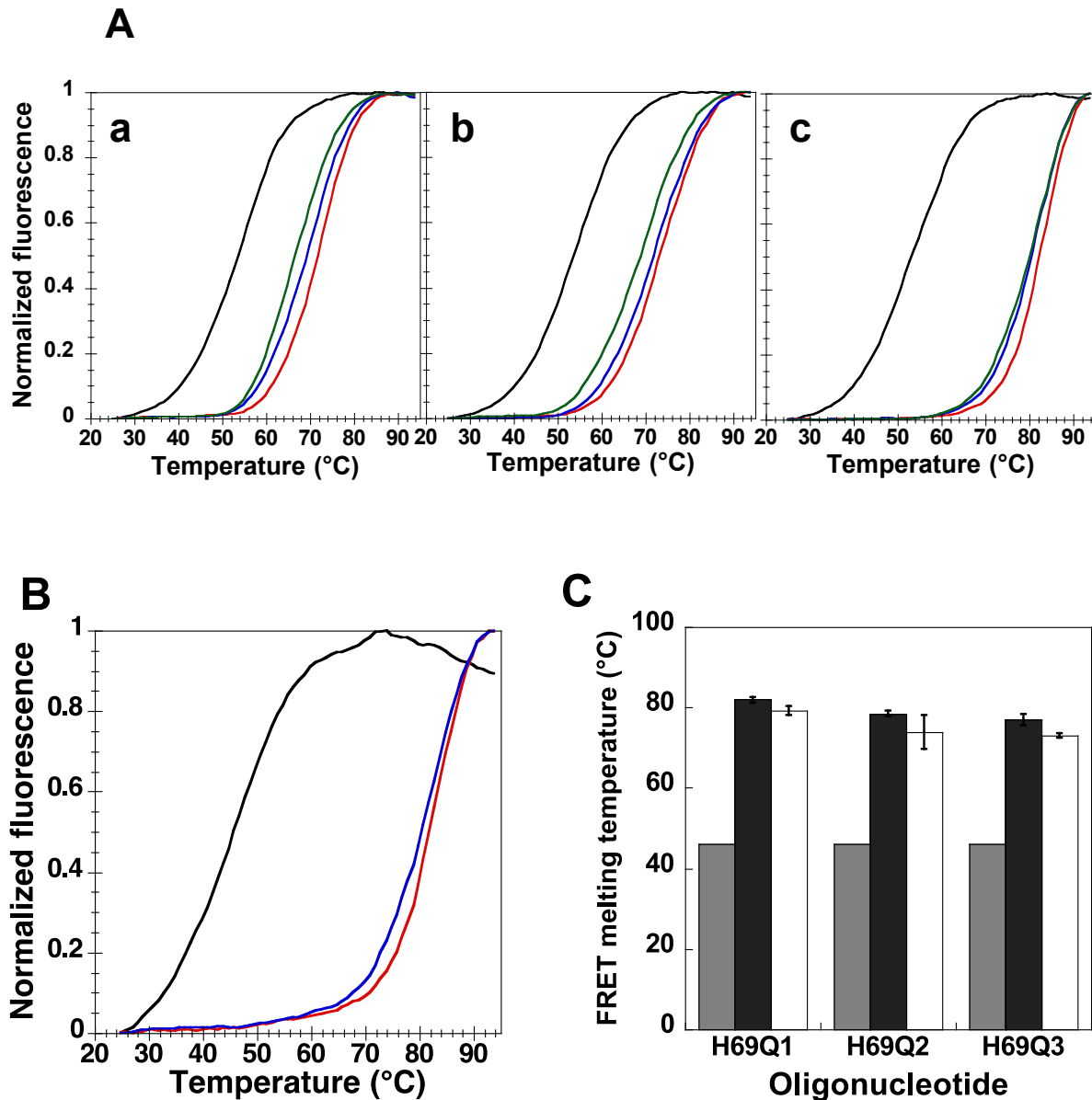


**Fig. S1** (A) FRET melting curves of F21T (black) in the presence of (a) 1  $\mu$ M of 360A, (b) 0.5  $\mu$ M and (c) 1  $\mu$ M of (360A)<sub>2A</sub>, without (red) or with 3  $\mu$ M (blue) or 10  $\mu$ M (green) of double-stranded competitor ds26. (B) Representative FRET melting curves of H69Q1 (black) in the presence of 1.5  $\mu$ M of (360A)<sub>2A</sub> without (red) or with (blue) 10  $\mu$ M of double-stranded competitor ds26. (C) FRET melting temperatures of H69Q1, H69Q2 and H69Q3 in the absence (grey bars) and in presence of 1.5  $\mu$ M of (360A)<sub>2A</sub> without (black bars) or with 10  $\mu$ M (white bars) of ds26. Errors bars are standard deviation on triplicate.

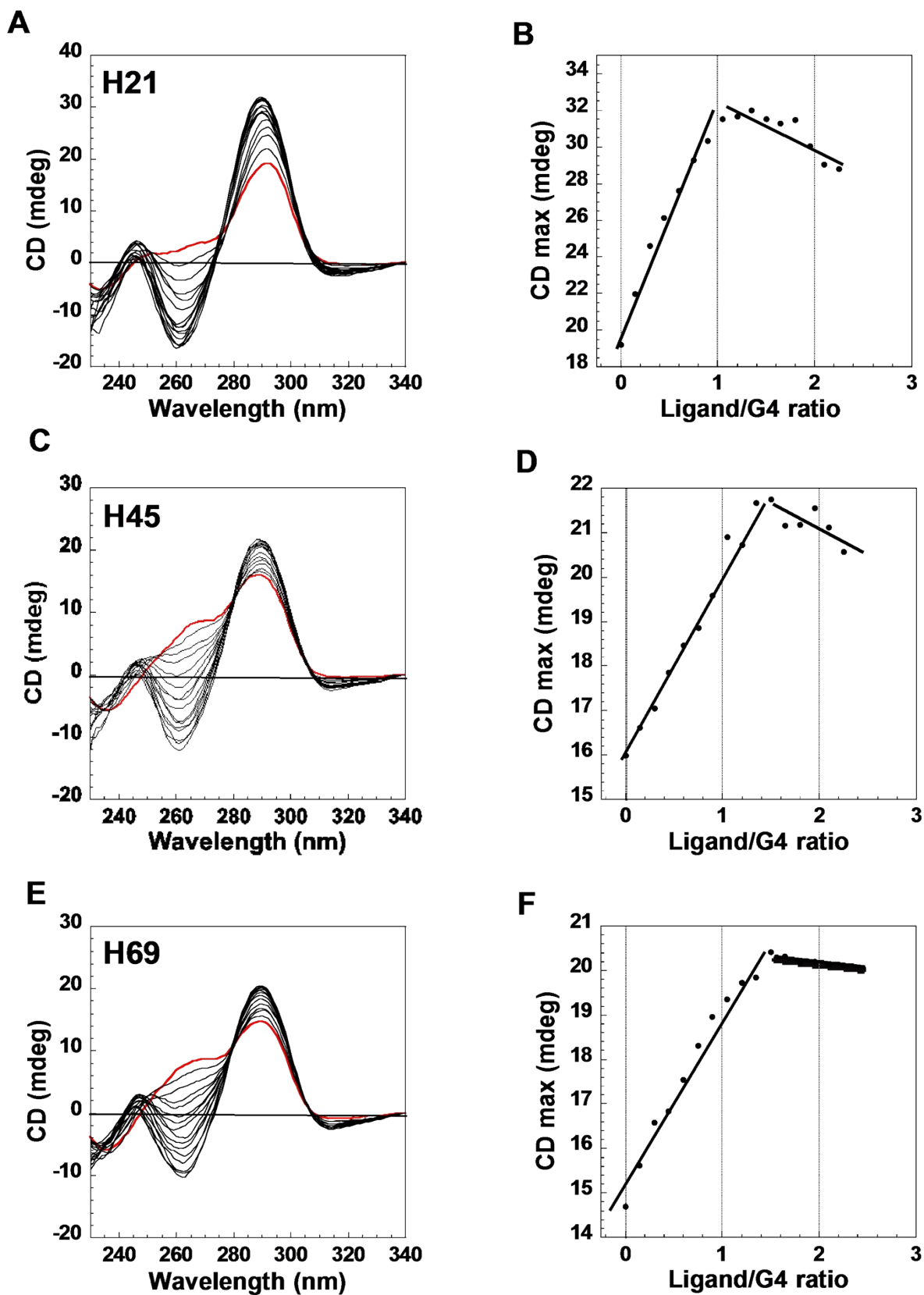


**Fig. S2** (A,C and E) Changes in the CD spectra and (B, D and F) changes in the maximum CD values of H21 (6  $\mu$ M), H45 (3  $\mu$ M) and H69 (2  $\mu$ M) upon addition of increasing amounts of (360A)<sub>2A</sub> in 10 mM lithium cacodylate pH 7.2, 10 mM KCl, 90 mM LiCl. The CD spectra in the absence of the ligand are in red.

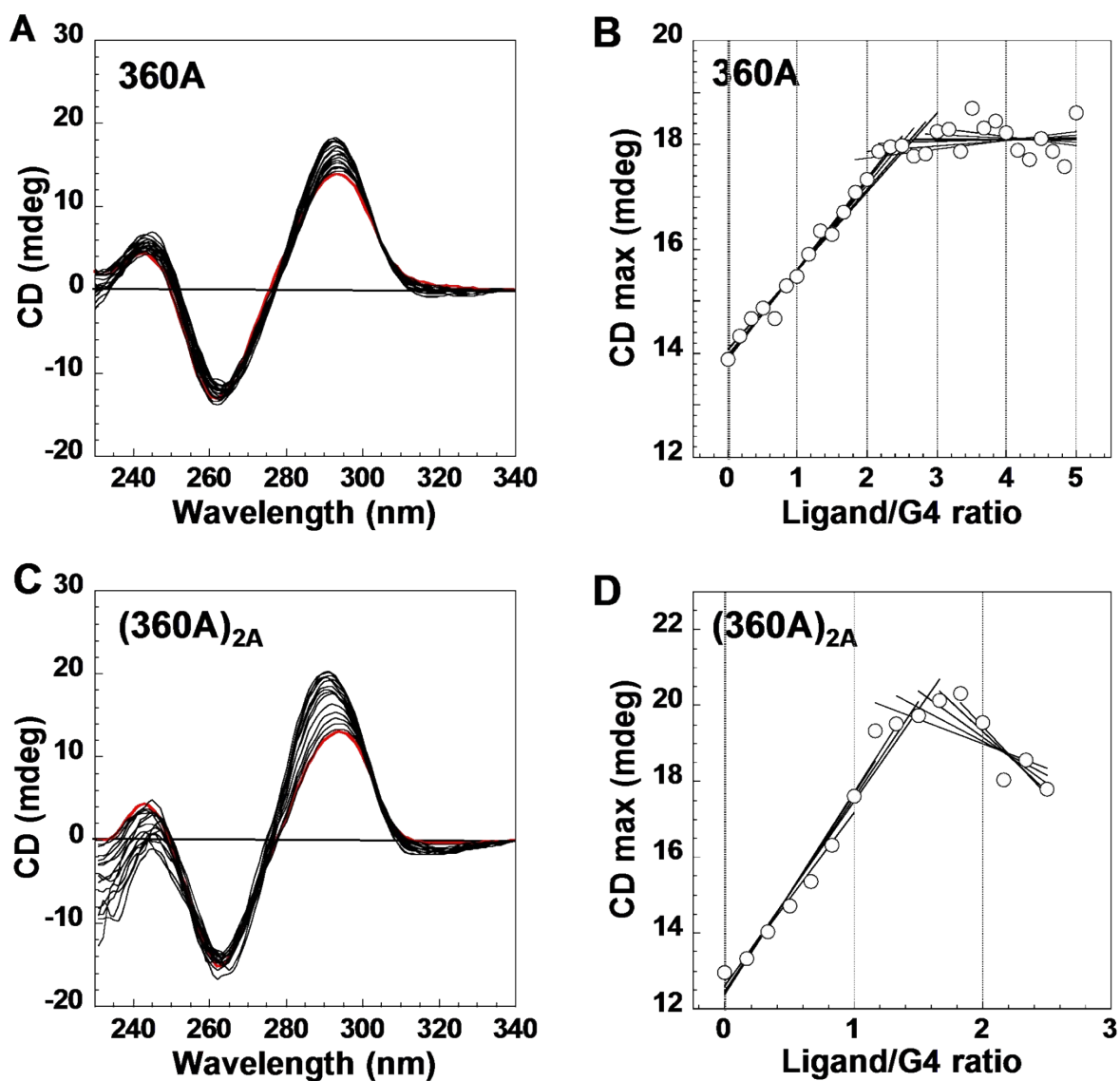


**Fig. S3** (A and C) Changes in the CD spectrum and (B and D) changes in the maximum CD value of H45 (3  $\mu$ M in 10 mM lithium cacodylate pH 7.2, 100 mM NaCl) upon addition of increasing amounts of 360A and (360A)<sub>2A</sub>. The CD spectrum without ligand is in red.

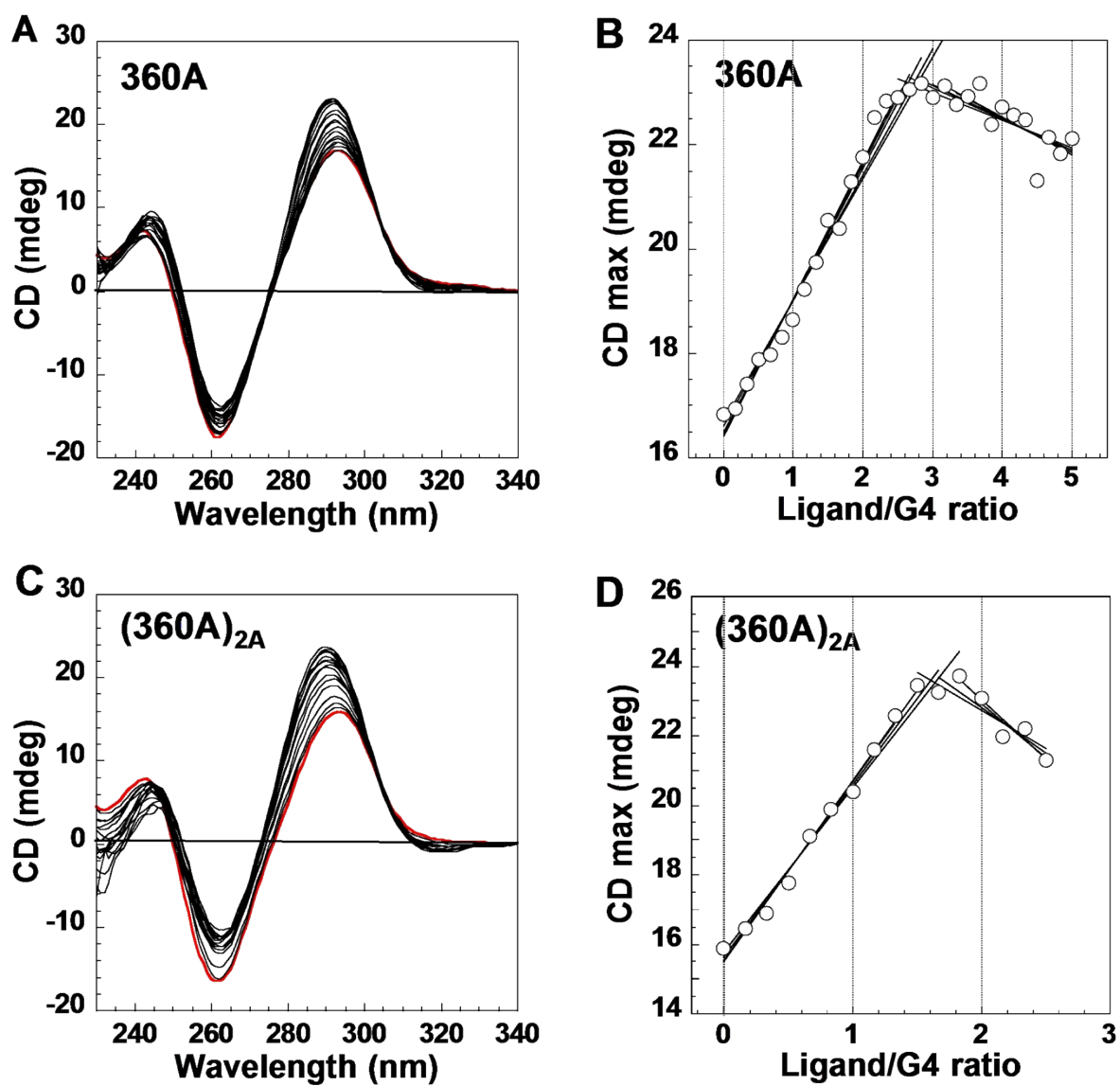


**Fig. S4** (A and C) Changes in the CD spectrum and (B and D) changes in the maximum CD value of H93 (1.5  $\mu$ M in 10 mM lithium cacodylate pH 7.2, 100 mM NaCl) upon addition of increasing amounts of 360A and (360A)<sub>2A</sub>. The CD spectrum without ligand is in red.

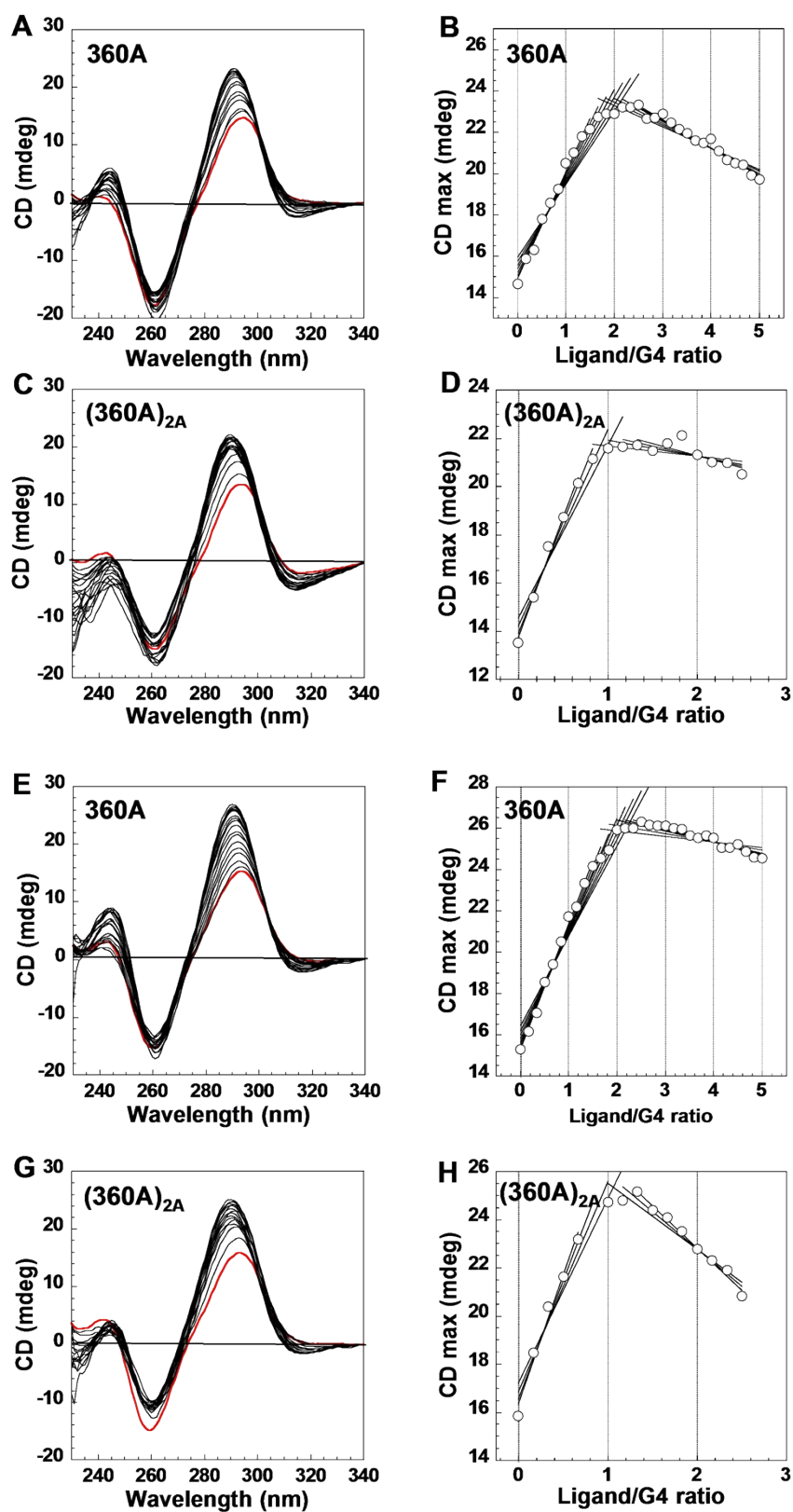


**Fig. S5** Changes in the CD spectra and in the maximum CD values of (A-D) H45(TTA)<sub>3</sub> (3  $\mu$ M) and (E-H) H69(TTA)<sub>3</sub> (2  $\mu$ M) upon addition of increasing amounts of 360A and (360A)<sub>2A</sub> in 10 mM lithium cacodylate pH 7.2, 100 mM NaCl. The CD spectra in the absence of the ligands are in red.

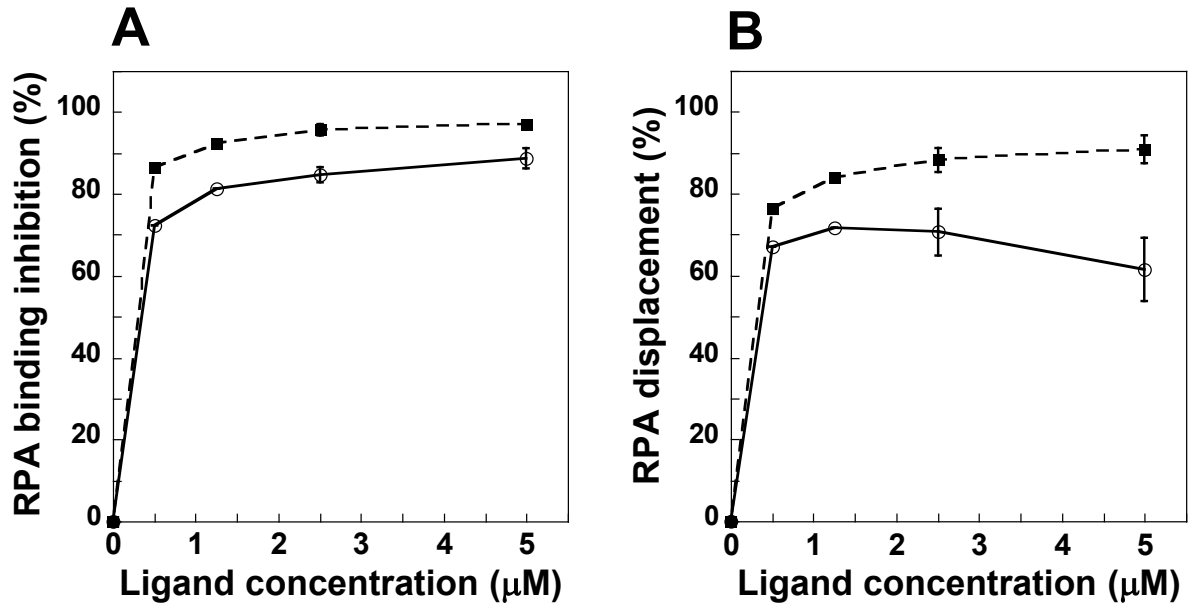


**Fig. S6** (A) Percentage of inhibition of RPA binding to telomeric oligonucleotide substrate H45 in the presence of increasing concentrations of 360A (open circles) or (360A)<sub>2A</sub> (black squares) for 5 min prior to incubation with RPA for 20 min. (B) Percentage of displacement of RPA from the telomeric oligonucleotide substrate H45 (20 min incubation) upon addition of increasing amounts of 360A (open circles) or (360A)<sub>2A</sub> (black squares) for 5 min.

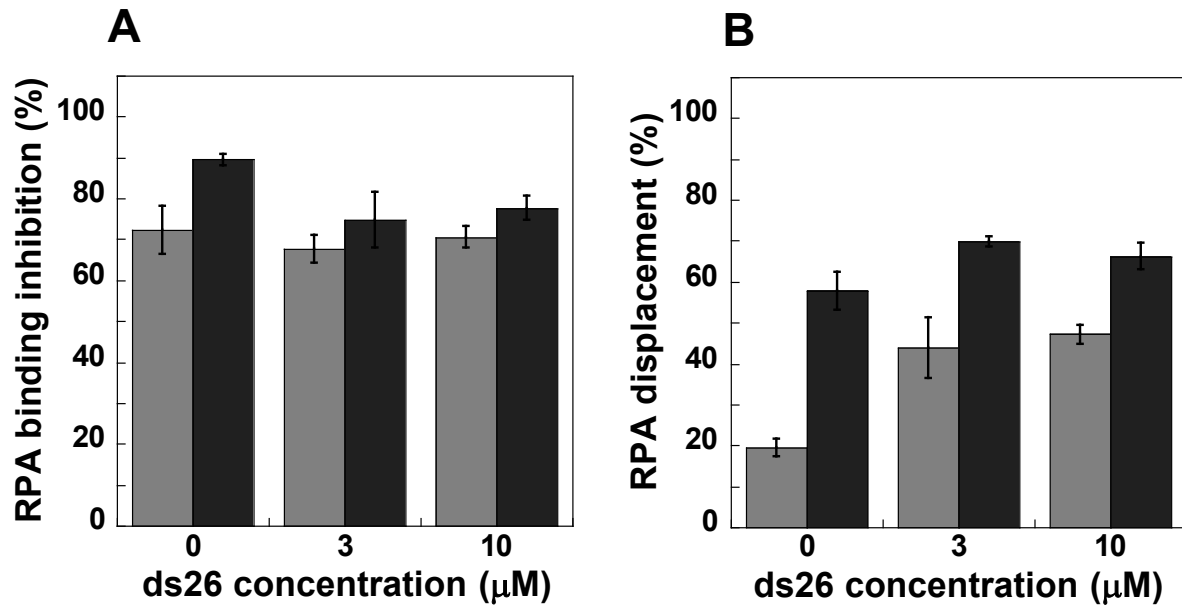


**Fig. S7** (A) Percentage of inhibition of RPA binding to telomeric oligonucleotide substrate H69 with 5  $\mu\text{M}$  of 360A (grey bars) or 2.5  $\mu\text{M}$  of (360A)<sub>2A</sub> (black bars) for 5 min in the presence of double-stranded competitor ds26 prior to incubation with RPA for 20 min. (B) Percentage of displacement of RPA from the telomeric oligonucleotide substrate H69 (20 min incubation) in the presence of double-stranded competitor ds26 upon addition of 5  $\mu\text{M}$  of 360A (grey bars) or 2.5 (360A)<sub>2A</sub>  $\mu\text{M}$  (black bars) for 5 min.

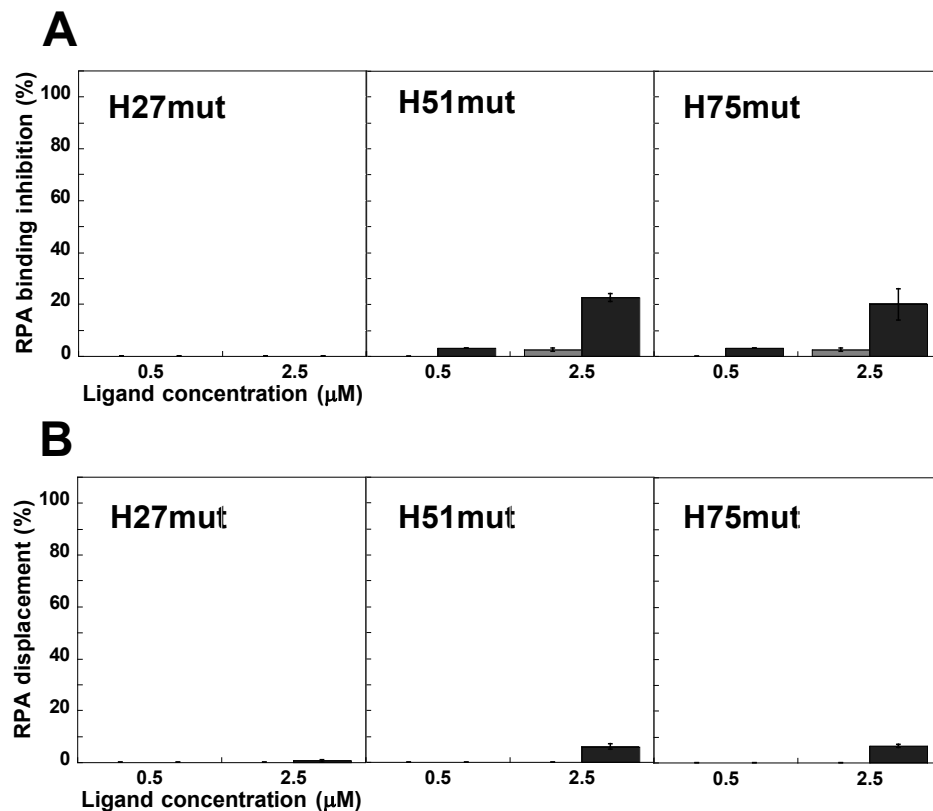


**Fig. S8** (A) Percentage of inhibition of RPA binding to mutated telomeric oligonucleotide substrates H27mut, H51mut and H75mut in the presence of increasing concentrations of 360A (grey bars) or (360A)<sub>2A</sub> (black bars) for 5 min prior to incubation with RPA for 20 min. (B) Percentage of displacement of RPA from the mutated telomeric oligonucleotide substrates H27mut, H51mut and H75mut (20 min incubation) upon addition of increasing amounts of 360A (grey bars) or (360A)<sub>2A</sub> (black bars) for 5 min.

## **Materials and methods**

### **Oligonucleotides**

Reverse-phase HPLC-purified oligonucleotides were purchased from Eurogentec (Belgium). They were dissolved in bi-distilled water and stored at -20°C. Concentrations were determined by UV absorption in bi-distilled water, using the molar extinction coefficients provided by the manufacturer.

### **Biochemical reagents**

BSA was purchased from Roche,  $\gamma$ -<sup>32</sup>P-ATP was from PerkinElmer Life Sciences and T4 polynucleotide kinase was from New England Biolabs. Recombinant hRPA was expressed in the *E. coli* BL21 (DE3) strain transformed with plasmid pET<sub>11a</sub>-hRPA that affords co-expression of RPA1, RPA2 and RPA3 subunits. The protein complex was purified as previously described.<sup>S1</sup>

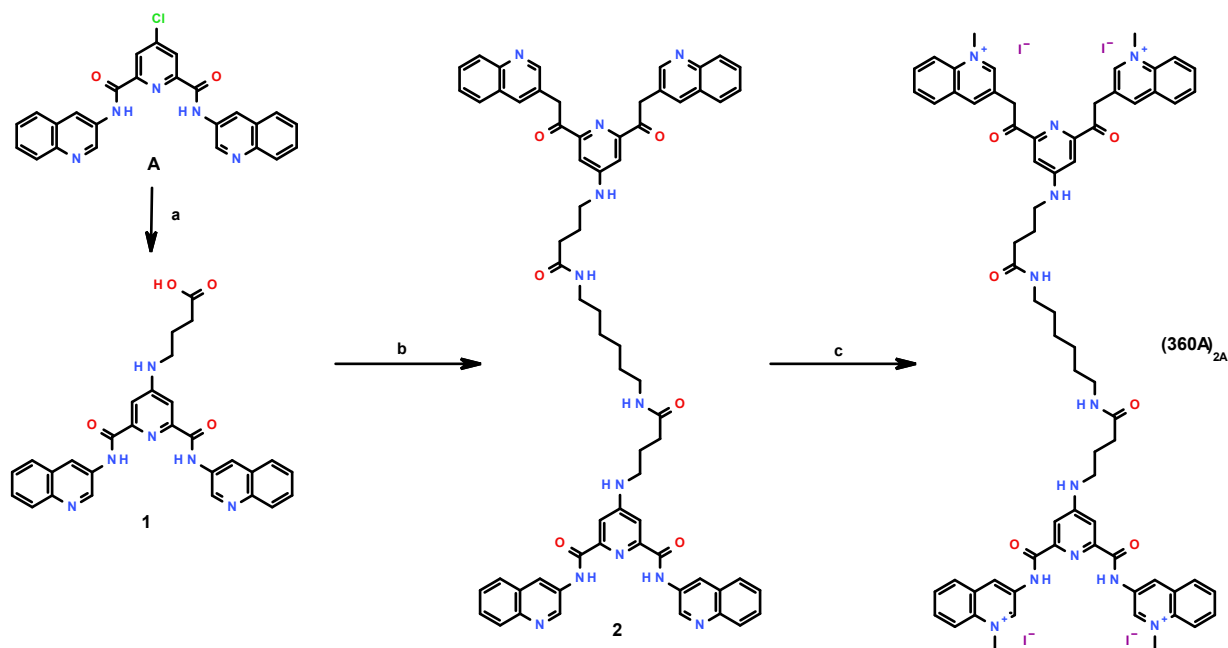
### **Chemical reagents and instrumentations**

Chemical reagents were purchased from Sigma-Aldrich and Fluka. Solvents were obtained from Carlo Erba. They were used without additional purification. Microwave heating was performed in a microwave synthesis reactor Monowave 300 (Anton Paar). Reverse-phase HPLC analysis and purification were performed on Agilent Technologies 1200 analytical and preparative apparatus piloted by an Agilent ChemStation program. In analytical HPLC standard conditions, compounds were analysed using a 25 min linear gradient of 0-to-100% water-acetonitrile-0.1% TFA on an analytical (4.6 x 250 mm) Kinetecs C18 EVO 5  $\mu$ m column (Phenomenex) at the flow rate of 1 mL.min<sup>-1</sup>, with detection by UV-absorption at both 260 and 310 nm. Reverse-phase preparative HPLC purifications were performed on a Waters column (Xbridge C18 5  $\mu$ m, 19 x 250 mm) using a 25 min linear gradient of 0-100% water-acetonitrile, containing 0.1% TFA, and monitored by UV detection at both 260 and 310 nm. Mass spectrometry analysis by ESI Q-TOF was performed on a Q-Star instrument (Applied Biosystems) in the positive mode; analyses were performed in methanol or DMF. NMR spectra were recorded on a Bruker AVANCE 400 NMR spectrometer equipped with a <sup>1</sup>H broad-band reverse gradient probehead. Stock solutions of the ligands (5 mM) were prepared in DMSO and stored at -20°C.

### **Chemical synthesis**

Synthesis of 360A molecule was carried out as previously described.<sup>S2</sup>

The dimer ligand (360A)<sub>2A</sub> was prepared with a 32% overall yield following the three-step process depicted below.



a) 4-aminobutyric acid / TEA / 2.5 h microwave heating in DMF at 140°. b) hexane-1,6-diamine / EDCI / HOBt / 4 days at room temperature in DMF. c) excess methyl iodide / 4 h microwave heating in DMF at 110°.

#### 4-[2,6-bis(quinolin-3-yl)aminocarbonyl-pyridin-4-yl]aminobutyric acid (**1**):

To a solution of 136 mg (0.3 mmol) of N<sub>2</sub>,N<sub>6</sub>-(quinolin-3-yl)-4-chloro-pyridine-2,6-dicarboxamide in DMF (5 mL) were added 34 mg (0.33 mmol) of 4-aminobutyric acid and 42  $\mu$ L (0.3 mmol) of triethylamine. After 2.5 h heating at 140°C in a microwave reactor and dilution with water (5 mL), the resulting colloidal mixture was centrifuged for 15 min at 4000 rpm. The solid was washed by centrifugation with 50% aqueous DMF (2 mL) and twice with water (10 mL), then dried 50°C under vacuum, yielding 72 mg (46%) of almost pure (**1**), as an off-white powder (m.p. > 260°C).

Rt (in standard analytical HPLC conditions) = 16.8 min.

<sup>1</sup>H NMR (400MHz, DMSO)  $\delta$  (ppm) = 12.3-12.5 (1H, bs), 11.4 (2H, s), 9.4 (2H, s), 8.95 (2H, s), 8.05 (4H, m), 7.8 (2H, s), 7.65 (2H, m), 7.55 (2, m), 5.6 (m, 1H), 4.35 (m, 2H), 2.4 (m, 2H), 1.65 (m, 2H).

SM (ESI-Q-TOF): [M+H]<sup>+</sup> = 521.45.

#### 1,6-{4-[2,6-bis(quinolin-3-yl)aminocarbonyl-pyridin-4-yl]amino-butanoyl}hexane-1,6-diamine (**2**):

62.5 mg (120  $\mu$ mol) of (**1**) and 15 mg (65  $\mu$ mol) of hexane-1,6-diamine were dissolved in dry DMF (2 mL). 23 mg (120  $\mu$ mol) of 1-ethyl-3-(3-dimethylaminopropyl)carbodiimide (EDCI) and 3.4 mg (25  $\mu$ mol) of 1-hydroxybenzotriazole (HOBt) were then added. After 4 days stirring at room temperature the yellow solution was diluted with water (2 mL). The white colloidal precipitate formed was separated by centrifugation at 4000 pm for 15 min, washed with water and dried at 50°C under vacuum. The crude product, dissolved in DMF, was purified by reverse-phase preparative HPLC in the conditions previously described and yielded 57 mg (85%) of (**2**) as a white solid (m.p. > 260°C).

Rt (in standard analytical HPLC conditions) = 19.5 min.

SM (ESI-Q-TOF): [M+H]<sup>+</sup> = 1121.21.

#### 1,6-{4-[2,6-bis(1-methyl-quinolinio-3-yl)aminocarbonyl-pyridin-4-yl]amino-butanoyl}hexane-1,6-diamine, tetra iodide ((**360A**)<sub>2A</sub>):

56 mg (50  $\mu$ mol) of (2) and 250  $\mu$ L (567 mg, 4 mmol) of methyl iodide were dissolved in DMF (1.5 mL) and heated at 110°C for 4 h in a microwave reactor. By cooling at room temperature, crystals separated that were filtered-off, washed successively with DMF (2 x 0.2 mL), ethanol (2 x 0.5 mL) and diethyl ether (2 x 2 mL) and dried, yielding 67 mg (79%) of pure (360A)<sub>2A</sub>, as bright yellow crystals.

Rt (in standard analytical HPLC conditions) = 18.7 min.

SM (ESI-Q-TOF): [M+2H]<sup>2+</sup> = 589.60; [M+H]<sup>+</sup> = 1179.21.

## Spectroscopic measurements

Oligonucleotide samples were prepared in a 10 mM cacodylic acid buffer at pH 7.2 in bi-distilled water (adjusted with LiOH), containing 100 mM NaCl or 10 mM KCl plus 90 mM LiCl, and placed in quartz cells (Hellma) with an optical pathway of 1 cm.

CD spectra were recorded on a J-810 spectropolarimeter (Jasco) at 20°C, after annealing of the oligonucleotide samples by heating at 95°C on a heat block, followed by a slow cool down to room temperature. Measurements were carried out in quartz cells (Hellma) with an optical pathway of 1 cm. CD spectra were obtained by averaging three scans at a scanning rate of 500 nm.min<sup>-1</sup>. They were baseline corrected by subtracting the spectrum of a water filled quartz cell and zero corrected at 340 nm. Titration experiments were performed by incremental additions of 3  $\mu$ L of a 180  $\mu$ M ligand solution, prepared in a 1X ad hoc buffer from a 5 mM stock solution in DMSO, in a 540  $\mu$ L oligonucleotide solution. CD signal amplitudes were corrected for the dilution factor resulting from ligand additions.

UV-melting profiles were recorded on an Uvikon XL spectrophotometer (Secomam) equipped with a circulating water bath (Julabo) and a dry airflow in the sample compartment. Samples were heated at 95°C for 2 min, cooled down at 5°C, and then heated back at 95°C, at a rate of 0.2°C.min<sup>-1</sup>. UV absorbance was recorded at 245, 260, 273, 295 and 335 nm every 5 min. Temperature was measured with a glass sensor immersed into a water filled quartz cell. Melting temperature (*T<sub>m</sub>*) was obtained as the maximum of the first derivative of the melting profile recorded at 273 nm.

## FRET melting experiment

FRET melting experiments were performed in 96-well plates with F21T (*FAM-G<sub>3</sub>[T<sub>2</sub>AG<sub>3</sub>]<sub>3</sub>-Tamra*, with *FAM*: 6-carboxyfluorescein and *Tamra*: 6-carboxytetramethylrhodamine) and three modified H69 oligonucleotides, doubly labelled with FAM and a TAMRA at different : in H69Q1, the fluorophores are placed at both sides of the first (5') G4 unit, in H69Q2, they are placed at both sides of the second G4 unit and in H69Q3, they are placed at both sides of the third (3') G4 unit. Fluorescence melting curves were recorded with a Mx300P real-time PCR instrument (Stratagene), using a total reaction volume of 25  $\mu$ L, with 0.2  $\mu$ M of oligonucleotide in a 10 mM cacodylic acid buffer at pH 7.2 in bi-distilled water (adjusted with LiOH) containing 100 mM NaCl. After a first equilibration step at 25°C during 5 min, a stepwise increase of 1°C for 70 cycles to reach 95°C was performed and measurements were made done after each cycle with excitation at 492 nm and detection at 516 nm. The melting of the G-quadruplex was monitored alone or with the ligands 360A or (360)<sub>2A</sub>, and in the absence or in the presence of double-stranded competitor ds26 (Table S1).

## RPA binding assays

Oligonucleotides were labelled with  $\gamma^{32}$ P-ATP using T4 polynucleotide kinase. They were separated from non-incorporated  $\gamma^{32}$ P-ATP through Biospin 6 columns (Biorad) according to the manufacturer's protocol. Prior binding experiments, stock solutions of hRPA

were diluted and pre-incubated 10 min at 4°C in a buffer containing 50 mM Tris-HCl, pH 7.5, 100 mM KCl, 1 mM DTT, 10% glycerol, 0.2 mg/mL BSA and 0.1 mM EDTA.

Binding experiments were carried out in 10 µl samples prepared in a reaction buffer containing 50 mM HEPES, pH 7.9, 0.1 mg/mL BSA, and 100 mM NaCl and 2% glycerol. For the first set of experiments, radiolabeled oligonucleotides (2 nM) were first incubated for 5 min at room temperature (~ 20°C) with various amounts of G4 ligands (0, 1.25, 2.5 or 5 µM final concentrations) before addition of RPA (100-200 nM final concentration), and further incubation for 20 min at room temperature. In the displacement conditions, radiolabeled oligonucleotide substrates were first incubated with RPA for 20 min at room temperature prior to addition of the G4 ligands, and further incubation for 5 min. For experiments in the presence of double-stranded competitor ds26 (Table S1), the competitor was added at the same time as the radiolabeled oligonucleotide substrate.

Samples were then loaded on native 1% agarose gels prepared with 0.5X TBE buffer. Electrophoresis was performed in 0.5X TBE running buffer for 90 min at 5 V/cm at room temperature in. Gel was then dried and exposed to a storage phosphor screen that was scanned with Typhoon™ FLA 95000 biomolecular imager (GE Healthcare). Band intensities ( $I$ ) were quantified using ImageQuant 5.2. For each G4 ligand concentration, the fraction ( $F$ ) of radiolabeled oligonucleotide substrate bound to RPA was calculated as  $I_{\text{oligo bound}} / (I_{\text{oligo bound}} + I_{\text{oligo free}})$  and the RPA binding inhibition or displacement as  $(F0 - Fc) / Fc$ , where  $F0$  is the fraction of oligonucleotide bound in the absence of the ligand and  $Fc$  the fraction bound in the presence of the ligand at the indicated concentration. Experiments were performed at least twice, with error bars representing the standard error on the mean.

## References

- S1 J. Audry, L. Maestroni, E. Delagoutte, T. Gauthier, T.M. Nakamura, Y. Gachet, C. Saintome, V. Geli, and S. Coulon, *EMBO J.*, 2015, **34**, 1942-1958.
- S2 A. Hittinger, T. Caulfield, P. Mailliet, H. Bouchard, E. Mandine, J. L. Mergny, L. Guittat, J. F. Riou, D. Gomez, C. Belmokhtar, WO2004/072027.